Magnetic-electron Compton profiles of ferromagnetic Fe and ferrimagnetic Mn ferrite

N. Sakai and H. Sekizawa*
The Institute of Physical and Chemical Research (RIKEN), Wako, Saitama 351-01, Japan
(Received 22 January 1987)

The magnetic-electron Compton profile of ferromagnetic polycrystalline Fe is investigated by using circularly polarized 129.5-keV γ rays from oriented ^{129m}Ir nuclei. In comparison with the band-theoretical magnetic-electron Compton profiles determined by means of the augmented-plane-wave or the linear combination of atomic orbitals methods, the experimental profile has a more negatively polarized momentum component around $p_z=0$ a.u. than do the theoretical ones, and a more positively polarized component above 5 a.u. The magnetic-electron Compton profile of ferrimagnetic polycrystalline Mn ferrite is measured for the first time. The observed profile resembles the Fe profile and also has a shallow dip around $p_z=0$.

I. INTRODUCTION

The energy spectrum of Compton scattered γ rays contains information on the electron-momentum distribution in matter. This spectrum gives the so-called Compton profile which is an integrated momentum distribution in a plane normal to the scattering vector. Up to this time, Compton profiles of metals such as Be (Refs. 1 and 2), Mg (Ref. 3), Al (Refs. 4 and 5), and Cu (Refs. 6 and 7) have shown that the band-theoretical calculations based on the one-electron approximation can reproduce the momentum distributions fairly well. However, evident quantitative disagreements between the experiment and the theory still remain in these Compton profiles. In the case of Cu, the theoretical failures are ascribed to nonlocal exchange-correlation effects.[7]

In the case of $3d$ magnetic materials, it is important to measure the momentum distribution of magnetic electrons selectively in order to obtain information on spin polarization and further to suggest a way to improve the band theory. This spin-polarization measurement can be achieved by utilizing the spin-dependent Compton scattering of circularly polarized γ rays.

This paper reports studies of magnetic-electron Compton profiles on polycrystalline ferromagnetic Fe, and also on ferrimagnetic Mn ferrite. The magnetic-electron Compton profile of ferromagnetic Fe had previously been measured by one of the authors,[8,9] and qualitative agreement between the observed profile and the augmented-plane-wave (APW) band-theoretical Compton profile was found, including agreement on the negative spin polarization of the itinerant electrons having sp-like character. The statistical accuracy of the experiment, however, was not satisfactory. Later, a much better circularly polarized γ-ray source was developed,[10] and a more improved profile of Fe could be obtained by using this new γ-ray source. Very recently, circularly polarized synchrotron radiation (SR) was successfully utilized to measure the magnetic-electron Compton profile of Fe.[11] The SR result will be compared with the present one in Sec. III.

The profile of ferrimagnetic Mn ferrite was also measured for the first time with the purpose of elucidating the difference in character between the localized magnetic electrons in Mn ferrite and the itinerant electrons in metallic Fe.

II. THEORETICAL

Utilization of the spin-dependent Compton scattering in order to measure the momentum distribution of magnetic electrons in magnetic materials was first proposed by Platzman and Tzoar[12] from a theoretical point of view, and a simple relation between the scattering cross section and the Compton profile was derived. Later, Rennert, Carl, and Hergert[13] also deduced the same relation applying relativistic corrections to the nonrelativistic time-dependent theory. For completeness, we start from the derivation of the equation which connects the scattering intensity with the Compton profile.

When photons are scattered by electrons with a definite momentum $\mathbf{p}$, the transition rate can be expressed as[14]

$$R=\frac{2\pi}{\hbar}d_f\mathrm{Tr}[\rho^{\mathrm{el}}(\mathbf{p}')\rho_f^{\mathrm{ph}}M\rho^{\mathrm{el}}(\mathbf{p})\rho_i^{\mathrm{ph}}M^{\dagger}]\ , \tag{2.1}$$

where d_f is the density of the final states, $\rho^{\mathrm{el}}(\mathbf{p})$ and $\rho^{\mathrm{el}}(\mathbf{p}')$ are the density matrices for the initial and the final state of the electron, respectively, and ρ_i^{ph} and ρ_f^{ph} are those of the photon, respectively. The operator M is related to the matrix element of the interaction Hamiltonian between the photon and the electron.

In solids, the electron wave function is expressed in terms of a set of proper basis functions. Usually the Compton scattering is described in terms of plane waves. Therefore, it is adequate for the present purpose to express the electron wave function by a superposition of plane waves. We should recall that the momentum component p_z of the initial electron is fixed after we measure the energy of the scattered photon. Here the z axis is parallel to the direction of the scattering vector of the photon. Therefore, differentiated by the energy of the scattered photon, the scattering cross section by the νth electron can be formulated as

$$\frac{d^2\sigma_\nu}{d\Omega\, dE_f}=\frac{2\pi}{\hbar}\int\int |f_\nu(\mathbf{p})|^2 df \times \mathrm{Tr}[\rho^{\mathrm{el}}(\mathbf{p}')\rho_f^{\mathrm{ph}} M \rho^{\mathrm{el}}(\mathbf{p})\rho_i^{\mathrm{ph}} M^\dagger]_\nu \times \delta(\mathbf{k}_i+\mathbf{p}-\mathbf{k}_f-\mathbf{p}')dp_x dp_y \ ,$$

where E_f is the energy of the scattered photon, $|f_\nu(\mathbf{p})|^2$ is the probability that the νth electron has a momentum $\mathbf{p}$, and $\mathbf{k}_i$ and $\mathbf{k}_f$ are the momenta of the initial and the final photon, respectively. The explicit expression of the density matrix $\rho^{\mathrm{el}}(\mathbf{p})$ is

$$\rho^{\mathrm{el}}(\mathbf{p})=\frac{1}{4}\left[1-\frac{c\mathbf{p}}{E}\cdot\zeta\rho_1-\frac{mc^2}{E}\rho_3+\mathbf{K}\cdot\boldsymbol{\sigma}-\frac{c\mathbf{p}}{E}\cdot\rho_1\boldsymbol{\sigma}+\frac{c\mathbf{p}\times\zeta}{E}\cdot\rho_2\boldsymbol{\sigma}+\mathbf{J}\cdot\rho_3\boldsymbol{\sigma}\right] ,$$
$$\mathbf{K}=\frac{mc^2}{E}\zeta+\frac{c^2\mathbf{p}(\mathbf{p}\cdot\zeta)}{E(E+mc^2)} \ , \qquad (2.2)$$
$$\mathbf{J}=-\zeta+\frac{c^2\mathbf{p}(\mathbf{p}\cdot\zeta)}{E(E+mc^2)} \ ,$$
$$E=(c^2p^2+m^2c^4)^{1/2} \ .$$

Here, ζ is the polarization vector of the electron, $\boldsymbol{\sigma}$ is the Pauli matrix, and ρ's are Dirac matrices. It is allowable to neglect the terms which contain p/mc, because in ordinary electron states, the main amplitudes of $f_\nu(\mathbf{p})$ exist within the momentum range from 0 to 10 a.u. (atomic units), whereas $mc=137$ a.u. The density matrix under this approximation becomes

$$\rho^{\mathrm{el}}(0)=\tfrac{1}{4}(1-\rho_3+\zeta\cdot\boldsymbol{\sigma}-\zeta\cdot\rho_3\boldsymbol{\sigma}) \ . \qquad (2.3)$$

This is exactly the density matrix of an electron at rest. If we assume that the electron final state is well represented by a single plane wave and that the polarization of the scattered photons are not observed, we get a relation between the Compton scattering cross section and the Compton profile $J(p_z)$ with the spin-dependent terms being included,

$$\frac{d^2\sigma}{d\Omega\, dE_f}=\frac{2\pi}{\hbar}df\,\mathrm{Tr}[\rho^{\mathrm{el}}(\mathbf{p}')\rho_f^{\mathrm{ph}} M \rho^{\mathrm{el}}(0)\rho_i^{\mathrm{ph}} M^\dagger] \times\sum_\nu\int\int |f_\nu(\mathbf{p})|^2 dp_x dp_y = \left[\frac{d\sigma}{d\Omega}\right]_{\mathrm{LT}} J(p_z) \ ,$$
$$J(p_z)=\sum_\nu\int\int |f_\nu(\mathbf{p})|^2 dp_x dp_y \ , \qquad (2.4)$$

where $(d\sigma/d\Omega)_{\mathrm{LT}}$ is the Compton scattering cross section calculated by Lipps and Tolhoek[14]

$$\left[\frac{d\sigma}{d\Omega}\right]_{\mathrm{LT}}=4r_0^2\left[\frac{E_f}{E_i}\right]^2(\Phi_0+\Phi_1+\Phi_2) \ ,$$
$$\Phi_0=\frac{1}{8}\left[(1+\cos^2\theta)+\frac{k_i-k_f}{mc}(1-\cos\theta)\right] \ ,$$
$$\Phi_1=\tfrac{1}{8}P_l\sin^2\theta \ ,$$
$$\Phi_2=-\tfrac{1}{8}P_c(1-\cos\theta)\zeta\cdot\frac{(\mathbf{k}_i\cos\theta+\mathbf{k}_f)}{mc} \ .$$

In these equations, r_0 is the classical electron radius, θ is the scattering angle, and P_l and P_c are the degree of linear and circular polarization of the incident photons, respectively. Since only the last term Φ_2 changes its sign on reversing the direction of the electron spin ζ, the following expression is obtained:

$$\left[\frac{d^2\sigma}{d\Omega\, dE_f}\right]^+-\left[\frac{d^2\sigma}{d\Omega\, dE_f}\right]^-=2J_{\mathrm{mag}}(p_z)\Phi_2^+ \ ,$$

where the symbols + and − denote spin up and spin down, respectively, and $J_{\mathrm{mag}}(p_z)$ is the *magnetic-electron* Compton profile,

$$J_{\mathrm{mag}}(p_z)=\sum_\nu\int\int[|f_\nu^+(\mathbf{p})|^2-|f_\nu^-(\mathbf{p})|^2]dp_x dp_y \ . \qquad (2.5)$$

This result shows that a simple relation holds between the spin-dependent Compton scattering intensity and the magnetic-electron Compton profile within the accuracy of the order of p/mc. If the cross section is calculated using the exact electron density matrix (2.2), a slightly momentum-dependent factor will be multiplied to the right-hand side of Eq. (2.4). This factor has been calculated by Ribberfors[15] for the case of the spin-*independent* scattering using a different formulation, but no calculation is available for the case of spin-dependent scattering.

When the γ-ray energy is around 100 keV as is the present case, its Compton scattering is not sensitive to the orbital angular momentum; the γ rays have wavelengths too short in comparison with the size of the electron orbit, and the magnetic interaction with the electron orbital motion is reduced to zero.

III. EXPERIMENTAL RESULTS AND DISCUSSION

Circularly polarized 129.5-keV γ rays were obtained from nuclear-oriented radioactive ^{191}Os nuclei embedded in iron. The half-life of this radioactive isotope is 15 d. The nuclear orientation was achieved by using a ^{3}He-^{4}He dilution refrigerator having a cooling power of 20 μW at 100 mK. The experimental details have already been reported.[10] The specimens of Fe and of Mn ferrite were polycrystals, and had the same size of $10\times5\times1$ cm^3. The scattering angle chosen was $145°\pm4°$. The energy spectra of the scattered γ rays were measured by a pure Ge solid-state detector having an energy resolution of 510 eV at 129 keV, and were stored in 1024-channel memory groups of a multichannel pulse-height analyzer.

A. Fe metal

Energy spectra of the Compton-scattered γ rays are shown in Fig. 1. The upper half of the figure is the spin-

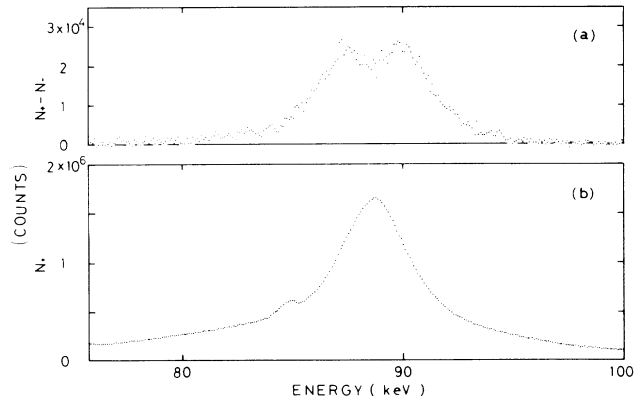

FIG. 1. Energy spectra of the Compton scattered γ rays by Fe. (a) The spin-dependent scattering obtained by subtracting the spin-down spectrum from the spin-up spectrum. (b) The spin-up total scattering.

dependent Compton scattering spectrum and the lower half is the total scattering one. The overall measuring time was 594.24 h, and three Os γ-ray sources were used consecutively. Corrections for (i) sample absorption, (ii) the Compton cross section, (iii) the long tail, and (iv) the multiple scattering should be made to the spin-dependent spectrum. Among them, the correction for the multiple scattering is the most important. The background correction is not needed for the spin-dependent spectrum, because the background, which is believed to be spin independent, is canceled out after subtracting the spin-down spectrum from the spin-up one. A computer simulation was made on the spin-dependent double scattering,[16] and the result is shown in Fig. 2. In the calculation, the spin-dependent Compton scattering cross section and the momentum distribution of electrons are fully considered, and the magnetic-electron momentum distribution was tentatively approximated by a Gaussian with a dip represented by an inverted Gaussian. The amount of the double scattering is 8.5% at the peak position, as can be seen from Fig. 2. The simulated total intensity ratio of the spin-dependent single scattering to the spin-dependent double one is 1:0.134. The corrections for the triple and further higher-order scatterings are estimated to be negligible.

After the corrections were made, the Compton peak in a momentum scale was folded at $p_z=0$ and averaged, and thus the magnetic-electron Compton profile shown in Fig. 3 was obtained. The statistical accuracy of the present profile is much improved in comparison with the previous one.[9] The solid line is the smoothed profile obtained by a 21-point smoothing procedure. The profile denoted by open circles is the recent SR Compton profile by Cooper *et al.*[11] The area is normalized to the present profile in a range from 0 to 6.4 a.u. The dashed curve is the theoretical magnetic-electron Compton profile calculated by Callaway and Wang[17] using the linear combination of atomic orbitals (LCAO) method based on the von Barth–Hedin exchange-correlation potential. The dotted curve is the one by Wakoh and Kubo[18] using the APW method based on modified spin-dependent $X\alpha$ potentials. The theoretical profiles are convoluted with a Gaussian having a full width at half maximum of 1.05 a.u., and the areas are normalized to the experimental one.

Comparisons between the various profiles will be made on the following three points: (1) the half-width at half maximum (HWHM) of the profile, which characterizes the overall feature of the profile, (2) the dip around $p_z=0$ a.u., which is explained by the theory to be due to the inverse polarization of electrons having *sp*-like character, (3) the high-momentum region above $p_z=4$ a.u., where the electron-lattice interaction and the electron-electron many-body interactions are liable to be observed.

The central dip and the high-momentum component above 4 a.u. (deeper and larger, respectively, than indicated in the theories) can be noticed in both experimental profiles. However, the HWHM of the SR profile is wider than the present γ-ray profile, and the maximum peak position shifts slightly to the higher momentum. The reason for these disagreements is not clear.

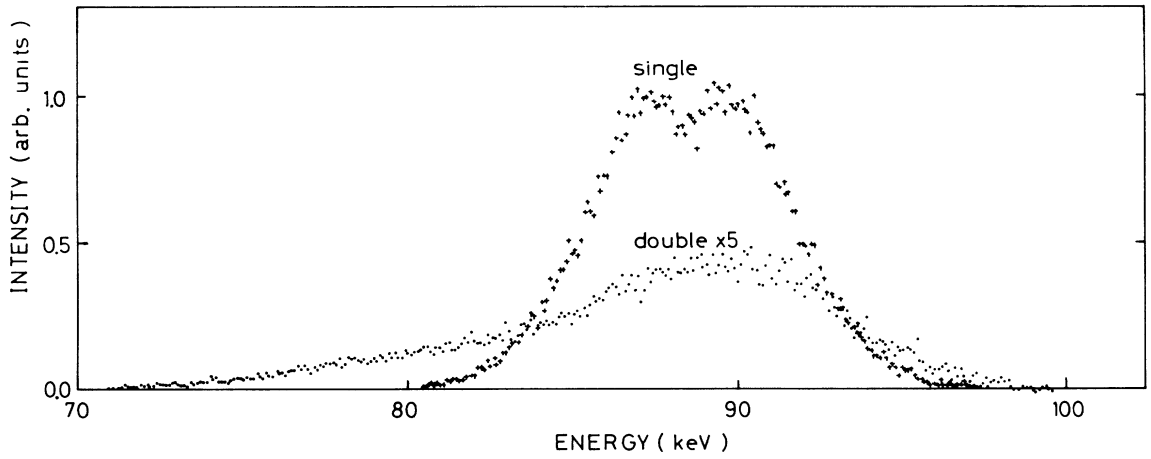

FIG. 2. Computer-simulated spin-dependent energy spectra of Fe for single Compton scattering (+) and for double scattering (· · ·).

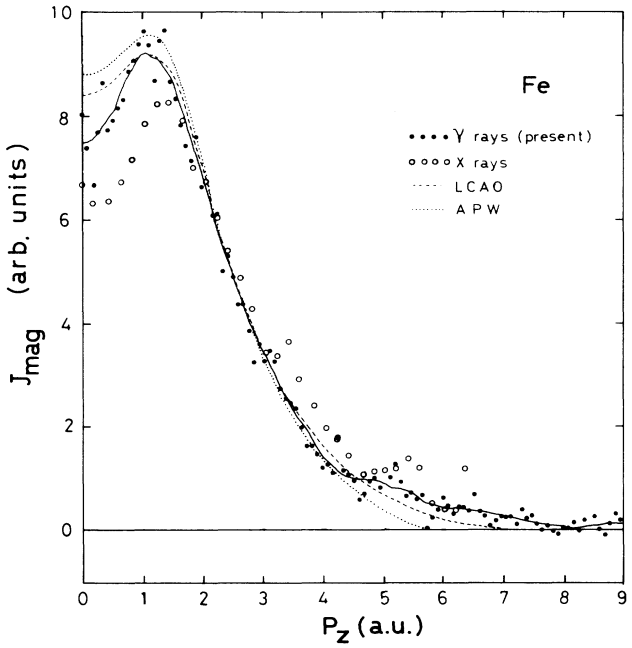

FIG. 3. Magnetic-electron Compton profile of polycrystalline ferromagnetic Fe metal. The spin-dependent profile in Fig. 1(a) is averaged from left to right after the corrections mentioned in the text. The solid line is the experimental profile smoothed by a 21-point procedure. The open circles are the profile (Ref. 11) using synchrotron radiation. The dashed line is the LCAO profile (Ref. 17) and the dotted line is the APW profile (Ref. 18), which are convoluted with the experimental resolution function.

A good agreement is found between the HWHM of the present γ-ray profile and the theoretical ones. It should be mentioned that the tail region of the APW profile is slightly narrower than the LCAO profile. A similar feature can also be noticed in the total-electron Compton profile.[18] This feature is one of the most significant differences between the APW profile and the LCAO one.

The experimentally observed dip is evidently deeper than the theoretical ones. The observed amount of the dip is 1.7 times as large as the LCAO value. According to the band theory, this dip is caused by the negative spin polarization of *sp*-like electrons hybridized with the 3*d* electrons. Since the hybridization depends on the orbital state of the electrons, the orbital state-dependent potentials for the 3*d* electrons seem to be effective in increasing the negative spin polarization of the electrons having *sp*-like character. However, if we compare the result of the APW calculation (which adopted $d\varepsilon$ and $d\gamma$ potentials) with that of the LCAO calculation (which adopted no state-dependent potentials), the amount of the dip is not much different from each other. Therefore, the state-dependent potentials are not effective in increasing the negative spin polarization of the *sp*-like electrons, and some improvement should be made in the band calculation to further clarify the origin of the negative spin polarization around $p_z=0$. The band calculations mentioned above do not include the effect of the spin-orbit coupling, which hybridizes the up-spin band and the down-spin band.[19] Thus, it is expected that inclusion of this effect will affect the magnetic-electron Compton profile. To examine this point, an experiment on a single crystal is highly desirable, because the spin orientation relative to the crystalline axes is explicitly defined in the theoretical calculation.

There is a systematic deviation of the theoretical profile from the experimental one in the region above 5 a.u. One possible explanation of this discrepancy is the effect of electron-electron correlations which are not sufficiently taken into account in the theoretical calculations. Nevertheless, the good agreement between the experimental magnetic-electron Compton profile and the theoretical one shows the present state of achievement of the band theory based on the one-electron approximation.

The momentum distribution of magnetic electrons in ferromagnetic Fe has been studied by the spin-polarized positron annihilation (PA) method.[20] The excellent agreement between the experiment and the theory reported in the PA study makes a noticeable contrast to the disagreement between the experiment and the theory found in the present Compton study. This is explained by the difference in characters of quantity appearing in these two studies. Contrary to the present Compton-profile analysis, the PA analysis was made on the difference angular correlations $n(\theta)=N_+(\theta)-N_-(\theta)$, where the total counts of $N_+(\theta)$ was normalized to that of $N_-(\theta)$. Moreover, the PA probability is proportional to the product of the positron wave function and the electron wave function. On the other hand, the Compton profile is given by the electron wave function only, as can be seen in Eq. (2.5). Thus, $n(\theta)$ is different in character compared with $J_{\rm mag}(p_z)$ of Eq. (2.5). It should be mentioned that the PA method measures the restricted momentum region $p_z<3$ a.u. as a result of the Coulomb repulsion between the positron and the nuclei. However, the 3*d* electrons have considerable momentum components above 3 a.u., and at that point the Compton method has revealed the disagreement between the experimental profile and the theoretical one.

B. Mn ferrite

It is interesting to compare the magnetic-electron Compton profile of metallic Fe with that of an insulator. From the experimental point of view, it is of course desirable to use a specimen with a high Curie temperature and a large magnetic moment. Among many magnetic insulators, ferrimagnetic Mn ferrite, $MnFe_2O_4$, was chosen because of its fairly large magnetic moment. Moreover, large Mn ferrite specimens are easily obtainable. The electric resistivity of this ferrite at room temperature is about 100 times higher than that of Fe metal. The site preference in this ferrite is, however, slightly complicated. There are two sites, *A* (tetrahedral) and *B* (octahedral), for metallic ions; *A* sites are occupied by 0.8 Mn^{2+} ions and 0.2 Fe^{3+} ions, and *B* sites are occupied by 1.8 Fe^{3+} ions and 0.2 Mn^{2+} ions.[21] Since the superexchange *B-B* interaction is ferromagnetic whereas the *A-B* interaction is antiferromagnetic, this ferrite has the magnetic moment of 1.6 Fe^{3+} ions subtracted by that of 0.6 Mn^{2+} ions. The

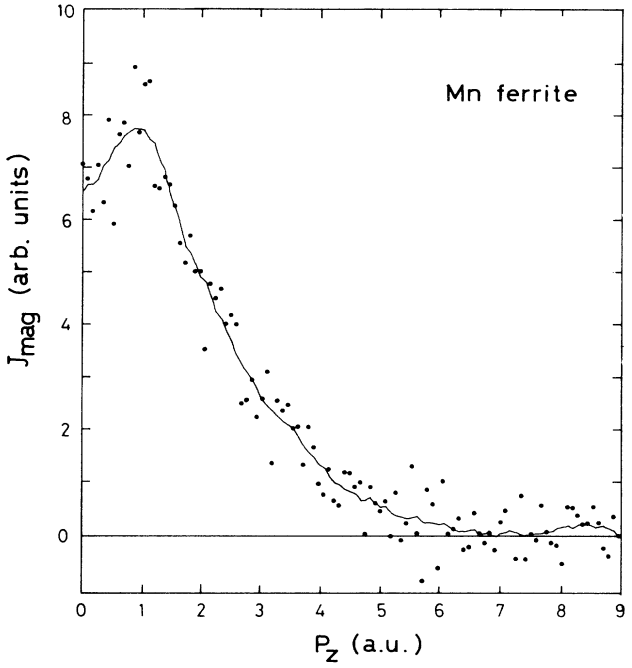

FIG. 4. Magnetic-electron Compton profile of polycrystalline ferrimagnetic Mn ferrite. The solid line is the experimental profile smoothed by a 21-point procedure.

ratio of the number of the magnetic electrons to the total is 0.038, which is only 44% of that of the ferromagnetic Fe. Thus, it is not easy to obtain a good magnetic-electron Compton profile of this ferrite in comparison with Fe. The observed magnetic-electron Compton profile is shown in Fig. 4. The accumulation time was 333.36 h. The various corrections similar to the ones described in the case of Fe are also made on this profile. Contrary to our expectation, the observed feature of the profile fairly well resembles that of metallic Fe; a shallow dip around $p_z=0$ a.u., and a similar width of the profile. The similar HWHM of this profile indicates that the spherically averaged radial distribution of the $3d$ electrons of this ferrite is almost equivalent to that of Fe metal. There is a possibility that the shallow dip observed in this ferrite originates partly from the different momentum distribution between Fe^{3+} and Mn^{2+}. The narrowness of the dip suggests that it is caused by the $3p$ or the $4s$ electrons. Unfortunately, no theoretical calculations of Compton profiles are available for this material.

IV. CONCLUSION

The magnetic-electron Compton profiles for ferromagnetic Fe and ferrimagnetic Mn ferrite were measured by using 129-keV circularly polarized γ rays from oriented ^{191m}Ir nuclei. The measurement of the magnetic-electron Compton profile for Fe could be achieved with high statistical accuracy, and the observed profile had a definitely deeper dip around $p_z=0$ a.u., and a longer tail beyond 5 a.u. than those of the theoretical profiles. These discrepancies between experiment and theory observed already in our previous work[8,9] were confirmed by the present work. The observed dip indicates that the amount of the negatively polarized electrons is 1.7 times larger than the theoretical value. Further improvement of the theoretical potentials taking electron-electron correlations and the spin-orbital coupling into account are desirable to clarify the origins of these discrepancies.

In spite of the completely different electronic structure, the observed magnetic-electron Compton profile of ferrimagnetic Mn ferrite resembles that of metallic Fe. The presence of a dip around $p_z=0$, which is shallower than that of Fe, is interesting. Since the momentum region of this dip is narrow, it seems reasonable to ascribe its origin to the $3p$, or the $4s$ electrons of Fe and Mn atoms.

The development of synchrotron radiation facilities makes it possible to examine not only the total electron structure but also the magnetic electron structure of $3d$ transition materials. In particular, the synchrotron radiation experiment will be advantageous for a small single crystal measurement because of the high brilliance of the radiation. On the other hand, the γ ray will be advantageous for the measurement of the Compton profiles of $4f$ and $5d$ elements, where low energy photons are strongly absorbed by the photo-electric effect.

ACKNOWLEDGMENTS

We greatly appreciate the deep interest Dr. N. Shiotani has shown in this study, and would like to thank Professor M. J. Cooper for sending his report on the Compton profile measurement using synchrotron radiation prior to publication.

*Present address: Chiba Institute of Technology, Narashino, Chiba 275, Japan.

[1]G. E. W. Bauer and J. R. Schneider, Solid State Commun. **47**, 673 (1983).
[2]M. Y. Chou, P. K. Lam, M. L. Cohen, G. Loupias, J. Chomilier, and J. Petiau, Phys. Rev. Lett. **49**, 1452 (1982).
[3]N. Sakai and H. Sekizawa, J. Phys. Soc. Jpn. **50**, 2606 (1981).
[4]P. Pattison, S. Manninen, J. Felsteiner, and M. Cooper, Philos. Mag. **29**, 973 (1974).
[5]F. Itoh, T. Honda, and K. Suzuki, J. Phys. Soc. Jpn. **46**, 1201 (1979).
[6]P. Pattison, N. K. Hansen, and J. R. Schneider, Z. Phys. B **46**, 285 (1982).
[7]G. E. W. Bauer and J. R. Schneider, Phys. Rev. Lett. **52**, 2061 (1984).
[8]N. Sakai and K. Ôno, Phys. Rev. Lett. **37**, 351 (1976).
[9]N. Sakai and K. Ôno, J. Phys. Soc. Jpn. **42**, 770 (1977).
[10]N. Sakai, O. Terashima, and H. Sekizawa, Nucl. Instrum. Methods **221**, 419 (1984).
[11]M. J. Cooper, D. Laundy, D. A. Cardwell, D. N. Timms, R.

S. Holt, and G. Clark, Phys. Rev. B **34**, 5984 (1986).
[12]P. M. Platzman and N. Tzoar, Phys. Rev. B **2**, 3556 (1970).
[13]P. Rennert, G. Carl, and W. Hergert, Phys. Status Solidi B **120**, 273 (1983).
[14]F. W. Lipps and H. A. Tolhoek, Physica (Utrecht) **20**, 85 (1954); **20**, 395 (1954).
[15]R. Ribberfors, Phys. Rev. B **12**, 2067 (1975); **12**, 3136 (1975).
[16]N. Sakai, J. Phys. Soc. Jpn. **56**, 2475 (1987).
[17]J. Callaway and C. S. Wang, Phys. Rev. B **16**, 2095 (1977).
[18]S. Wakoh and Y. Kubo, J. Magn. Magn. Mater. **5**, 202 (1977).
[19]M. Singh, C. S. Wang, and J. Callaway, Phys. Rev. B **11**, 287 (1975).
[20]P. E. Mijnarends, Physica **63**, 248 (1973).
[21]J. M. Hastings and L. M. Corliss, Phys. Rev. **104**, 328 (1956).